A LETTERS JOURNAL EXPLORING THE FRONTIERS OF PHYSICS

January 2020

EPL, **129** (2020) 15001
doi: 10.1209/0295-5075/129/15001

www.epljournal.org

Study on plasma ejection near the anode in a pulsed low-current vacuum discharge

JIA TIAN[(a)], WENZHENG LIU[(b)], YONGJIE GAO, WENJUN ZHANG, and LUXIANG ZHAO

School of Electrical Engineering, Beijing Jiaotong University - 100044, Beijing, China

received 15 September 2019; accepted in final form 21 January 2020
published online 11 February 2020

PACS 52.80.Vp – Discharge in vacuum
PACS 52.65.Cc – Particle orbit and trajectory
PACS 52.50.Dg – Plasma sources

Abstract – An electrode structure with two anodes, one of which is covered by an insulating material layer with a micropore, is proposed in this letter, and adopting this electrode structure enables a special vacuum discharge phenomenon, by which a visible ejected plasma jet is formed near the anode in a pulsed low-current (∼200 A) vacuum discharge to be firstly observed. According to experimental study and theory analysis, the formation mechanism of the discharge phenomenon observed above is analysed. Study on this special discharge phenomenon is of vital importance for revealing the basic physical processes in a vacuum discharge.

Introduction. – The metal plasma source produced by a vacuum discharge can be used for ion implantation, extraction of highly ionized ion beams, and pulsed plasma thrusters [1–6]. In a vacuum discharge, the physical processes near cathode and anode are of significance for metal plasma generation and motion characteristics [7,8]. It is recognized that the metal plasma is generated from cathode spots with a diameter of several micro-meters [9–11]. In terms of metal ion acceleration, according to the hump theory, all ions are assumed to move toward the anode under the action of the $\mathrm{Hump_c}$ potential near the cathode [12–15]. In addition, it is generally believed that, in a high-current vacuum discharge (over 1 kiloampere) where the morphology of the generated plasma is contracted, metal ions arriving at the anode bombard the anode, forming anode spots and releasing metal ions from the anode; while, in a low-current vacuum discharge (∼ a few hundred amperes), the anode just acts as a passive collector of particles emitted from the cathode [16–18].

In the research process of a vacuum arc thruster (VAT) applied to micro-satellites, it was found that a strong luminous region was formed near the anode and an ejected plasma jet perpendicular to the anode surface was generated. These special discharge phenomena cannot be well explained by using the existing vacuum discharge theory. The aim of this study is to explore the motion mechanism of plasma near the anode as well as the generation and propagation characteristics of the ejected plasma jet near the anode.

Experimental setup. – The two different electrode structures proposed in this study, electrode I and electrode II, and their parameters are shown in fig. 1. The electrode structure mainly consists of a lead cathode, a ceramic insulating sleeve and two anodes, a cylindrical proximal anode (PA) and a solid cylinder distant anode (DA). A conical cathode is arranged in the insulating sleeve. The PA, which mainly provides the electric field for electron emission, is sleeved on the outer surface of the insulating sleeve and completely covered by ethylene-vinyl acetate (EVA) insulating material. The DA, which is made of copper, is set in front of the insulating sleeve nozzle at a distance of 25 mm from the cathode tip which is the discharge end. The DA of structure I shown in fig. 1(a) is exposed. The DA surface of structure II shown in fig. 1(b) is wrapped by an EVA insulating material layer, in which a micropore of 1.0 mm in diameter is set at its geometric center, and charged particles generated during discharge can enter the DA through the micropore. All experiments were carried out in a grounded stainless steel vacuum chamber, and the pressure of the vacuum chamber was controlled at 10^{-4} Pa. The output voltage of the single-pulse power supply adopted ranged from 0 to −20 kV. Discharge voltage was measured by a high-voltage probe of Tektronix P6015A 1000×, which was connected to the

(a) E-mail: 17117424@bjtu.edu.cn
(b) E-mail: wzhliu@bjtu.edu.cn (corresponding author)

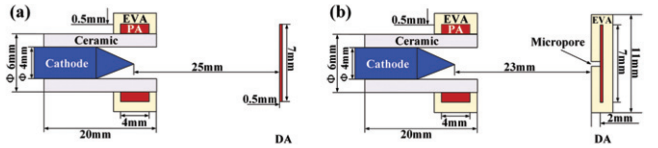

Fig. 1: Schematic of models and parameters of (a) electrode I and (b) electrode II.

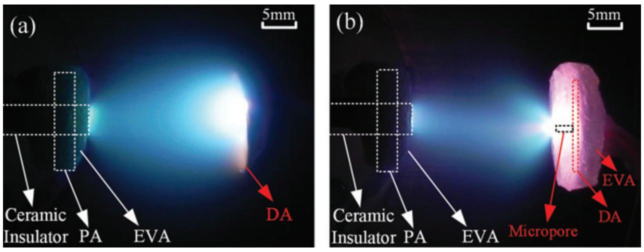

Fig. 2: Discharge images with an exposure time of 0.5 seconds by using (a) electrode I (b) electrode II.

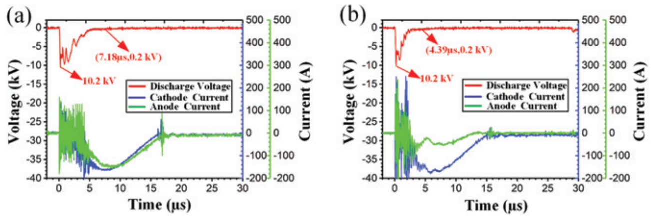

Fig. 3: Waveforms of discharge voltages and discharge currents by using (a) electrode I (b) electrode II.

lead-out line of the cathode. Discharge currents flowing through the cathode side (cathode current) and the anode side (anode current) were simultaneously measured by using two identical Rogowski coils, which were sleeved on the lead-out lines of cathode and anodes, respectively. Output signals of high-voltage probe and Rogowski coils were recorded by an oscilloscope Tektronix TBS 1154.

Results and discussions. – Because of the good insulating property of the high vacuum, when studying the characteristics of a vacuum discharge, the gap between cathode and anode of the electrodes adopted previously used to be set within a few millimeters, but it is difficult to observe detailed discharge processes near anode and cathode separately [19]. By using the electrode structures shown in fig. 1, the discharge phenomena near the anode can be clearly presented when the DA is 25 mm away from the cathode tip. Discharge images captured by a camera Nikon D7100 are shown in fig. 2. It is seen from fig. 2(a) that bright luminous regions are formed on the surface and in the near region of DA. Moreover, in this case, the whole discharge channel between cathode and DA is bright. In comparison, for the discharge morphology of electrode II shown in fig. 2(b), only near the micropore, a luminous region which is perpendicular to the DA surface and diffuses toward the cathode is formed; furthermore, brightness of the discharge channel is weaker, and there is no obvious luminescence on the surface of EVA insulating material layer except for the micropore.

The waveforms of discharge voltages, cathode currents and anode currents are shown in fig. 3. It is seen from fig. 3(a), for electrode I, that the amplitude of the cathode current is about 166.0 A and the anode current is almost equal to that of the cathode current. In comparison, for electrode II shown in fig. 3(b), the peak cathode current is about 179.0 A, but the anode current amplitude decreases sharply and just accounts for 28% of the cathode current. It is analysed that the difference between cathode current and anode current is the current formed by the plasma which diffuses from the insulating sleeve nozzle to the vacuum chamber and finally reaches the inside wall of the grounded vacuum chamber.

It is known that in a vacuum discharge, charged particles generated from cathode spots, including electrons and part of the ions, were eventually absorbed by the exposed anode [12,20–22]. However, it is seen from the discharge phenomena shown in fig. 2 that the luminescence intensities at the vicinity of the exposed parts of the anodes for the two electrode structures are all high.

It is inferred that this phenomenon is due to the smooth entry of electrons into the anode and accumulation of metal ions near the anode when plasma moves to the vicinity of the anode. Because there is a micropore on the EVA insulating material layer surface of the DA for the electrode structure II, a high positive space potential ($\mathrm{Hump_a}$ potential) similar to the $\mathrm{Hump_c}$ near the cathode is formed because of the metal ions gathering in front of the micropore, pushing the metal ions generated from the cathode to eject towards the cathode direction. As the metal ions ejecting towards the cathode hinder the plasma from moving towards the anode, the anode current is significantly reduced. Furthermore, after electrons enter the anode through the micropore, the electrons in the plasma channel move to the axial direction, and the metal ions also move axially at the same time under the action of the Coulomb force, leading to the phenomenon by which the luminescence on the EVA insulating material surface of the DA except for the micropore is not obvious.

According to fig. 2(b), the plasma jet ejected from the insulating sleeve nozzle and that ejected from the micropore on the EVA insulating material layer surface of DA overlap each other. In order to determine and verify the propagation direction of the plasma jet near the micropore, we removed the DA and set the micropore on the PA surface in the direction perpendicular to the cathode axis, and the discharge image is shown in fig. 4(a).

It is seen from fig. 4(a) that a diffused plasma jet which is ejected outwards is formed at the nozzle of the insulating sleeve, and a plasma jet is also generated near the micropore. Then, an improved Langmuir probe measurement

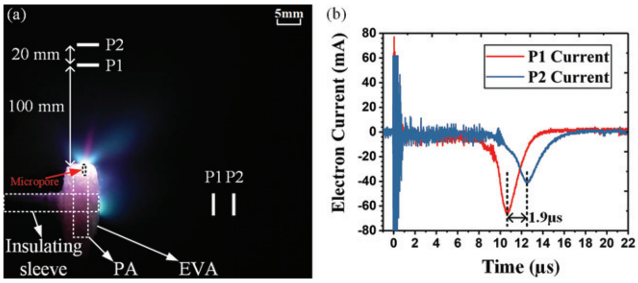

Fig. 4: (a) Discharge image when the micropore is arranged on the PA surface in the direction perpendicular to the cathode axis with an exposure time of 0.5 s. (b) The typical waveforms of electron currents flowing through the two Langmuir probes when applied bias voltages are all 8 V.

system was adopted to measure the propagation velocity of plasma jets [14,23]. First of all, two Langmuir probes with 20 mm interval were arranged in front of the micropore at the axial direction of 100 mm, as shown in fig. 4(a). Electron current waveforms flowing through the two probes are shown in fig. 4(b). It is seen from fig. 4(b) that the plasma jet first reaches probe 1 closer to the micropore and then arrives at the distant probe 2, suggesting that the plasma jet does not converge towards the micropore but ejects outwards from the micropore. In addition, due to the diffusion of plasma, the peak electron current in probe 1 is greater than that in probe 2. According to the time interval between the two probe current peaks, it is calculated that the plasma was ejected from the micropore at a speed of $1.05 \times 10^4\,\mathrm{ms}^{-1}$. By using the same measurement method, the waveforms of electron currents measured in the axial direction of the insulating sleeve are similar to those in the axial direction of the micropore, and the corresponding velocity of the plasma ejected from the insulating sleeve is $8.9 \times 10^3\,\mathrm{ms}^{-1}$.

It is analysed that, for the electrode II shown in fig. 2(b) and the electrode structure shown in fig. 4(a), the formation mechanism of plasma jets near the micropore is the same. Therefore, based on the discussion above, we think that the plasma jet generated near the anode in the case of structure II was also ejected outward from the micropore. Additionally, according to the electrical parameters shown in fig. 3, discharge currents of two electrode structures are all less than 200 A and plasma morphologies near anodes are all not contracted but diffused, indicating that it is impossible for the luminescence near the anode to be derived from the metal ions produced by the anode spots. It is speculated that both of the plasma jets near the micropore are formed by the positive space potential ($\mathrm{Hump_a}$) owing to the accumulation of metal ions.

Conclusion. – In conclusion, the special discharge phenomena of a strong luminous region near the anode and a visibly ejected plasma jet near the anode in a pulsed low-current discharge are firstly observed. Based on the assumption of hump theory, the formation mechanism of plasma jet near the anode is presented and analysed. This study provides support for further understanding the physical processes of a pulsed vacuum discharge and the improvement of ejection performance of metal plasma. Of course, the mechanism by which these special discharge phenomena occur still needs to be identified in great detail.

* * *

This work is supported by the Fundamental Research Funds for the Central Universities (No. 2018YJS162, China) and the National Natural Science Foundation of China (No. 51577011).

REFERENCES

[1] Öztarhan A., Brown I., Bakkaloglu C., Watt G., Evans P., Oks E., Nikolaev A. and Tek Z., *Surf. Coat. Technol.*, **196** (2005) 327.
[2] Nikolaev A. G., Yushkov G. Yu., Oks E. M., Oztarhan A., Akpek A., Hames-Kocabas E., Urkac E. S. and Brown I. G., *Appl. Surf. Sci.*, **310** (2014) 51.
[3] Bugaev A., Gushenets V., Yushkov G., Oks E., Kulevoy T., Hershcovitch A. and Johnson B. M., *Appl. Phys. Lett.*, **79** (2001) 919.
[4] Shipilova O. I., Chernich A. A. and Paperny V. L., *Phys. Plasmas*, **24** (2017) 103108.
[5] Keidar M., Schein J., Wilson K., Gerhan A., Au M., Tang B., Idzkowski L., Krishnan M. and Beilis I. I., *Plasma Sources Sci. Technol.*, **14** (2005) 661.
[6] Polk J. E., Sekerak M. J., Ziemer J. K., Schein J., Qi N. and Anders A., *IEEE Trans. Plasma Sci.*, **36** (2008) 2167.
[7] Boxman R. L., Sanders D. M. and Martin P. J., *Handbook of Vacuum Arc Science and Technology* (Noyes Publications, Park Ridge, NJ) 1995.
[8] Shkol'nik S. M., *Plasma Sources Sci. Technol.*, **20** (2011) 013001.
[9] Shao J. H., Antipov S. P., Baryshev S. V., Chen H. B., Conde M., Doran D. S., Gai W., Jing C. G., Liu W. M., Power J. *et al.*, *Phys. Rev. Lett.*, **115** (2015) 264802.
[10] Mesyats G. A., Bochkarev M. B., Petrov A. A. and Barengolts S. A., *Appl. Phys. Lett.*, **104** (2014) 184101.
[11] Djakov B. E. and Holmes R., *J. Phys. D: Appl. Phys.*, **7** (1974) 569.
[12] Plyutto A. A., Ryzhkov V. N. and Kapin A. T., *Sov. Phys. JETP*, **20** (1965) 328.
[13] Bolotov A., Kozyrev A. and Korolev Y., *IEEE Trans. Plasma Sci.*, **23** (1995) 884.
[14] Tian J., Liu W. Z., Cui W. S. and Gao Y. J., *Plasma Sci. Technol.*, **20** (2018) 085403.
[15] Shmelev D. L., Barengolts S. A. and Tsventoukh M. M., *IEEE Trans. Plasma Sci.*, **45** (2017) 3046.

[16] Dyuzhev G. A., Lyubimov G. A. and Shkolnik S. M., *IEEE Trans. Plasma Sci.*, **11** (1983) 36.
[17] Miller H. C., *IEEE Trans. Plasma Sci.*, **13** (1985) 242.
[18] Anders A., *Appl. Phys. Lett.*, **78** (2001) 2837.
[19] Heberlein J. V. R. and Gorman J. G., *IEEE Trans. Plasma Sci.*, **8** (1980) 283.
[20] Goldsmith S. and Boxman R. L., *J. Appl. Phys.*, **51** (1980) 3649.
[21] Beilis I. I., Keidar M., Boxman R. L. and Goldsmith S., *J. Appl. Phys.*, **83** (1998) 709.
[22] Neumann P. R. C., Bilek M. M. M., Tarrant R. N. and McKenzie D. R., *Plasma Sources Sci. Technol.*, **18** (2009) 045005.
[23] Tian J., Liu W. Z., Gao Y. J. and Zhao L. X., *Phys. Plasmas*, **26** (2019) 023511.